Evolution of low-temperature phases in a low-temperature structural transition of a La cuprate

Y. Inoue
Structural Analysis Section, Research Department, Nissan ARC Ltd., 1 Natsushima-cho, Yokosuka, Kanagawa 237, Japan

Y. Horibe
Department of Materials Science and Engineering, Waseda University, Shinjuku-ku, Tokyo 169, Japan

Y. Koyama
Kagami Memorial Laboratory for Materials Science and Technology, Waseda University, Shinjuku-Ku, Tokyo 169, Japan and Department of Materials Science and Engineering, Waseda University, Shinjuku-ku, Tokyo 169, Japan

(Received 8 April 1997)

The microstructure produced by a low-temperature structural phase transition in $La_{1.5}Nd_{0.4}Sr_{0.1}CuO_4$ has been examined by transmission electron microscopy with the help of imaging plates. The low-temperature transition was found to be proceeded not only by the growth of the $Pccn$/low-temperature-tetragonal phases nucleated along the twin boundary but also by the nucleation and growth of the phases in the interior of the low-temperature-orthorhombic domain. In addition, because the map of the octahedron tilt as an order parameter is not identical to that of the spontaneous strain accompanied by the transition, the microstructure below the transition is understood to be a very complex mixture of the low-temperature phases. [S0163-1829(97)02145-0]

The La cuprate $La_{2-x}Ba_xCuO_4$ with $x=0.125$ exhibits a low-temperature structural phase transition from a low-temperature-orthorhombic (LTO: space group $Bmab$) phase to a low-temperature-tetragonal (LTT: space group $P4_2/ncm$) one on cooling from a high-temperature-tetragonal (HTT: space group $I4/mmm$) one. It is well understood that the transition is characterized as a tilt of the CuO_6 octahedron in the crystal structure.[1,2] As for the physical properties, suppression of the superconducting temperature T_c has been reported in this oxide and the role of the low-temperature transition in this suppression is still under discussion.[1–4] In order to elucidate the relation between the physical properties and the transition, it is necessary to examine the microstructure related to the transition. Changes in the microstructure due to the low-temperature transition in La cuprates have not been studied sufficiently.

Chen *et al.* examined the microstructure of the LTT phases in both $La_{1.875}Ba_{0.125}CuO_4$ and Nd_2NiO_4 by transmission electron microscopy and found that there are antiphase boundaries with respect to oxygen-atom displacements related to the tilt of the CuO_6 octahedron.[5,6] They also pointed out on the basis of convergent-beam electron diffraction that the crystal symmetry is not uniformly tetragonal in a specimen, but changes from place to place.[6,7] That is, regions with an orthorhombic distortion are present locally in the LTT phase. On the other hand, Zhu *et al.* showed on the basis of their transmission-electron-microscopy observation that the LTT phase appears only along the twin boundary between the LTO domains.[8] In this case, however, the volume fraction of the LTT phase is estimated to be very small and is obviously not compatible with that determined from x-ray and neutron diffractions. In order to elucidate this discrepancy, we made *in situ* observations of the low-temperature phase transition in $La_{1.5}Nd_{0.4}Sr_{0.1}CuO_4$ by transmission electron microscopy. This oxide undergoes successive transitions from the LTO phase to a $Pccn$ one with orthorhombic symmetry and then to the LTT one.[9] One reason why we decided to examine the transitions in $La_{1.5}Nd_{0.4}Sr_{0.1}CuO_4$ is that this oxide has almost the highest transition temperature among the low-temperature transitions in the La cuprates.

The sample preparation of $La_{1.5}Nd_{0.4}Sr_{0.1}CuO_4$ has been described in our previous papers.[10,11] Specimens for transmission-electron-microscopy observation were prepared by an Ar-ion thinning technique. The *in situ* observation was performed by using a transmission electron microscope equipped with a cooling stage incorporating a liquid-He reservoir, in addition to a 5 μm objective aperture. Features of the low-temperature phase transition were examined by taking electron-diffraction patterns, bright-field images, and dark-field images at each temperature in a range between room temperature and 12 K. In the present work, dark-field images were recorded on imaging plates in order to avoid specimen drift during exposure. In contrast to a conventional film with an exposure time of about 90 s, we could take images only for about 3 s in the case of the imaging plate. Because the microstructure is entirely changed by aging for about 60 s, the use of the imaging plate is our advantage for clarifying the change in the microstructure during the low-temperature transition.

The structural phase transitions in the La cuprates are characterized by the tilt of the CuO_6 octahedron as an order parameter. In particular, the tilt axis of the octahedron deviates from the LTO tilt about the $\langle 110 \rangle$ direction in the low-temperature transition. As a result of the deviation, 100-type spots such as 100 and 010 spots appear in the electron-diffraction patterns of the $Pccn$ and LTT structures, while these spots are absent from the HTT and LTO structures. That is, the 100-type spots are unique to the product phases

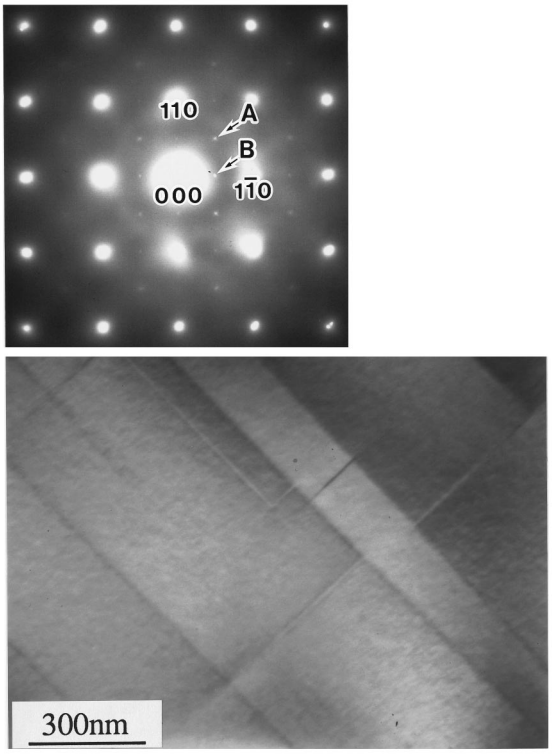

FIG. 1. Bright-field image of $La_{1.5}Nd_{0.4}Sr_{0.1}CuO_4$ at 85 K, together with the corresponding electron-diffraction pattern.

and absent in the parent phase in the low-temperature transition. Then we call the 100-type spot a unique spot. From these features, therefore we can check the occurrence of the low-temperature structural transition and examine the details of the microstructure in the transition by taking dark-field images using these unique spots. On the other hand, we cannot distinguish between these two structures on the basis of electron diffraction because both *Pccn* and LTT structures are detected only by the appearance of the unique spots. For that reason, we will refer to the *Pccn*/LTT structures here without making any distinction between them and define the LTO→*Pccn*/LTT transition as the low-temperature structural transition.

$La_{1.5}Nd_{0.4}Sr_{0.1}CuO_4$ was reported to undergo successive transitions from LTO→*Pccn*→LTT on cooling.[9] The transition temperature of the LTO-to-*Pccn*/LTT transition in the specimen used in the present experiment was determined to be about 120 K based on the appearance of the unique spots. Figure 1 shows a bright-field image of $La_{1.5}Nd_{0.4}Sr_{0.1}CuO_4$ at 85 K, together with the corresponding electron-diffraction pattern. The electron beam was parallel to the [001] direction and diffraction spots have been indexed in terms of the HTT structure. The diffraction pattern shows the presence of both fundamental spots due to the HTT structure and the unique 100-type spots, as indicated by arrow *A*. The latter spots indicate the presence of the *Pccn*/LTT phase. Note that 1/2, 1/2, 0-type superlattice spots are also observed in the pattern, as indicated by arrow *B*.[10] One notable feature of the bright-field image is the presence of a banded contrast. The same contrast was seen at room temperature in the LTO phase. That is, the contrast is identical to that due to the LTO domains which form a twin structure, although the image was taken at 85 K, well below the transition temperature of the low-temperature transition. In addition, the twin boundaries were confirmed to be parallel to the {100} planes.

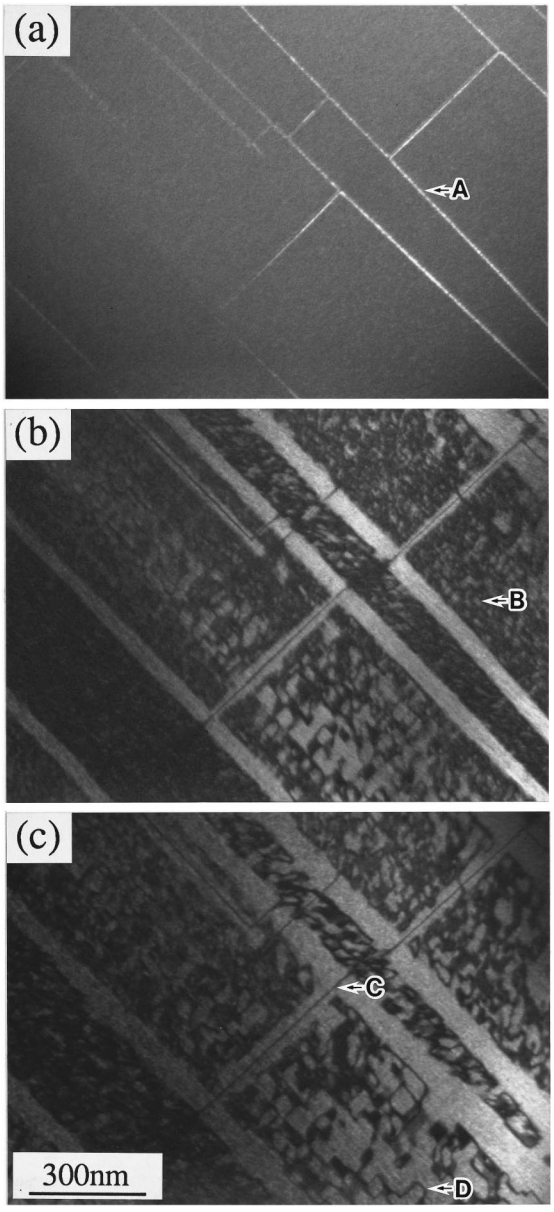

FIG. 2. 100 dark-field images of $La_{1.5}Nd_{0.4}Sr_{0.1}CuO_4$ at 85 K, (a), and 12 K, (b) and (c). Images (b) and (c) were taken from the sample kept at 12 K for 32 and 36 min, respectively.

In order to clarify the details of the microstructure, we made *in situ* observations of the low-temperature transition in $La_{1.5}Nd_{0.4}Sr_{0.1}CuO_4$ by taking dark-field images using the unique spot. Figure 2(a) is a 100 dark-field image at 85 K, which was obtained from the same area shown in Fig. 1. A bright-line contrast is clearly observed in the image, as indicated by arrow *A*. From a comparison with the bright-field image of Fig. 1, the line contrast *A* is found to exist along the twin boundary between the LTO domains. This implies that the *Pccn*/LTT phase appears along the twin boundary, as was found by Zhu *et al.*[8] In order to examine the change in the microstructure, we then cooled the specimen and kept it at 12 K. Figures 2(b) and 2(c) are 100 dark-field images at 12 K, which were taken from the specimen kept at 12 K for 32 and 36 min, respectively. As is seen in these figures, when

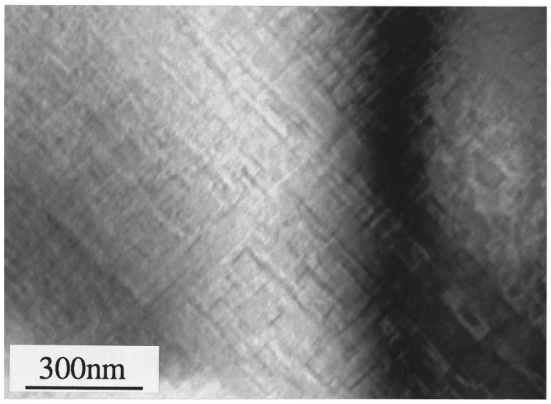

FIG. 3. 110 dark-field image of $La_{1.5}Nd_{0.4}Sr_{0.1}CuO_4$ at 12 K.

the specimen is kept at 12 K, the bright-line contrast changes to a banded contrast as a result of the widening of the line contrast. The most notable feature in Fig. 2(b) is that the bright-spotty contrast appears in the interior of the LTO domains, as indicated by *B*. On further aging at 12 K, the size of the bright-spotty contrast region increases, as seen in Fig. 2(c), together with the further widening of the bright-band contrast region along the twin boundary *A*. From a comparison between Figs. 2(b) and 2(c), the size of the spotty contrast region and the width of the band-contrast region were estimated to increase at rates of about 2 and about 3 nm/min, respectively. In addition, a boundary between the spotty contrast region and the LTO matrix can be understood to be characterized as an abrupt boundary. This is because a change in the contrast across the boundary is relatively sharp.

Let us interpret the origin of the contrasts found in the 100 dark-field images at 12 K. The contrast in the 100 dark-field image should be the diffraction contrast. The bright-spotty contrast region therefore has the *Pccn*/LTT structure, just like the band contrast region. The low-temperature transition is then understood to be characterized by the nucleation and growth of the *Pccn*/LTT phase in the interior of the LTO domain as well as by the growth of the phase nucleated along the twin boundary. In addition, a dark-line contrast can be seen inside the bright-band contrast, as indicated by *C*. The growth of the spotty-contrast region also results in a similar dark-line contrast in some areas, as indicated by *D*. It should be remarked that the features of the dark-field image shown in Fig. 2(c) are entirely the same as those reported by Chen *et al.*[5,6] As they observed, the dark-line contrast can be explained as being due to the antiphase boundary with respect to the tilt of the CuO_6 octahedron.

In order to examine the cause of these features described just above, we took fundamental dark-field images at 12 K. Figure 3 shows a dark-field image at 12 K, which was taken by using the 110 spot. The image shows the presence of the so-called ''tweed contrast'' running along the ⟨100⟩ directions over the entire area. The contrast is very similar to that observed in $YBa_2Cu_3O_{7-\delta}$, V_3Si, and metallic alloys.[12–21] According to previous studies of the tweed contrast, the contrast is understood to be due to a macroscopic strain. Recently Parlinski, Heine, and Salje pointed out that the macroscopic strain field giving rise to this contrast is produced by a local misfit of the neighboring strained unit cells.[12] That is, the spontaneous strain accompanied by the transition is not uniform in the specimen and varies from place to place. The most important fact to be noted here is that the map of the tweed contrast in Fig. 3 is not identical to that of the *Pccn*/LTT regions in the 100 dark-field image, which is precisely a region characterized by the *Pccn*/LTT tilt of the octahedron. In other words, there is no one-to-one correspondence between the order parameter and the spontaneous strain. We can therefore conclude that the microstructure below the low-temperature transition is a very complex mixture of the LTO and *Pccn*/LTT phases.

The present observation clearly indicates that the low-temperature phases—the LTO, *Pccn*, and LTT phases—coexist in a complex fashion below the transition temperature of the low-temperature transition in $La_{1.5}Nd_{0.4}Sr_{0.1}CuO_4$. The major feature of the microstructure is that the spotty-shape region with the *Pccn*/LTT tilt appears in the interior of the LTO domain, in addition to the band-shape region along the twin boundary. The low-temperature transition is therefore characterized not only by the growth of the *Pccn*/LTT phase nucleated along the twin boundary but also by the nucleation and growth of the phase in the interior of the LTO domain. These are the characteristic features of the low-temperature structural transition in the La cuprates.

A specimen with a thickness of ~100 nm; that is, a thick film, is usually used in transmission-electron-microscopy observation. This raises the question as to whether the observed microstructure is present in a bulk sample. Before a discussion of the characteristic features of the low-temperature transition, we should mention general aspects of a role of the sample geometry in the first-order transition. It is known that the first-order transition proceeds by the nucleation and growth of a product phase in a parent-phase matrix. The nucleation sites of the product phase have been understood to be a free surface, as well as structural defects such as a grain boundary. Particularly the surface plays a main role in the nucleation in the case of a single crystal. Even when a thickness of the specimen decreases, however the number of these sites involved in the specimen never increases remarkably. The nucleation itself must be therefore hardly affected by the sample geometry. Since the growth of the product phase is controlled by the degree of the relaxation of the transformation strain, the sample geometry is one of the important factors for the growth. That is, the transformation strain in a film is relaxed more easily than that in a bulk sample. The product phase can be then extended in a wider area in a thinner film. It can be eventually said that, because the degree of the relaxation changes continuously with respect to the thickness of the specimen, the microstructure found in our work should appear in the bulk sample. In other words, the present sample geometry promotes the progress of the low-temperature transition.

It is time to discuss the characteristic features of the low-temperature transition. The so-called tweed contrast seen in Fig. 3 reflects the map of the spontaneous strain accompanied by the transition. The very important fact is that there is disagreement between the map of the tilt of the octahedra as an order parameter and the spontaneous strain. It is obvious that the disagreement results in the aid of the nucleation and growth of the *Pccn*/LTT-tilt region in some areas but the

suppression of them in others. The disagreement is therefore concluded to stabilize the coexistence of the LTO and *Pccn*/LTT phases in a very complex fashion. Complex fashion means that locally there exist the LTO-tilt region with the *Pccn*/LTT strain and the *Pccn*/LTT-tilt region with the LTO strain in the specimen. This type of coupling between the order parameter and the strain can not be predicted on the basis of Landau theory. In other words, group theory is locally broken down in the low-temperature transition in the La cuprate.

In summary, the low-temperature phase transition in the La cuprate is characterized by the nucleation and the growth of the *Pccn*/LTT phase with a spotty shape in the interior of the LTO domain as well as by the growth of the phase nucleated along the twin boundary. Because the order parameter is not locally coupled to the appropriate spontaneous strain, the low-temperature phases coexist in the complex fashion below the transition temperature of the low-temperature transition, even at the lowest temperature obtained in the present work.

[1] J. D. Axe, A. H. Moudden, D. Hohlwein, D. E. Cox, K. M. Mohanty, A. R. Moodenbaugh, and Y. Xu, Phys. Rev. Lett. **62**, 2751 (1989).
[2] R. M. Fleming, B. Batlagg, R. J. Cava, and E. A. Rietman, Phys. Rev. B **35**, 7191 (1987).
[3] A. R. Moodenbaugh, Y. Xu, M. Suenaga, T. J. Folkerts, and R. N. Shelton, Phys. Rev. B **38**, 4596 (1988).
[4] T. Suzuki and T. Fujita, J. Phys. Soc. Jpn. **58**, 1883 (1989).
[5] C. H. Chen, D. J. Werder, S.-W. Cheong, and H. Takagi, Physica C **183**, 121 (1991).
[6] C. H. Chen, S.-W. Cheong, D. J. Werder, and H. Takagi, Physica C **206**, 183 (1993).
[7] C. H. Chen, S.-W. Cheong, D. J. Werder, A. S. Cooper, and L. W. Rupp, Jr., Physica C **175**, 301 (1991).
[8] Y. Zhu, A. R. Moodenbaugh, Z. X. Cai, J. Tafto, M. Suenaga, and D. O. Welch, Phys. Rev. Lett. **73**, 3026 (1994).
[9] M. K. Crawford, R. L. Harlow, E. M. McCarron, W. E. Farneth, J. D. Axe, H. Chou, and Q. Huang, Phys. Rev. B **44**, 7749 (1991).
[10] Y. Koyama, Y. Wakabayashi, S.-I. Nakamura, Y. Inoue, and K. Shinohara, Phys. Rev. B **48**, 9710 (1993).
[11] Y. Koyama, Y. Wakabayashi, K. Ito, and Y. Inoue, Phys. Rev. B **51**, 9045 (1995).
[12] K. Parlinski, V. Heine, and E. Salje, J. Phys.: Condens. Matter **5**, 497 (1993).
[13] A. Bratkovski, S. Marais, V. Heine, and E. Salje, J. Phys.: Condens. Matter **6**, 3679 (1994).
[14] S. Marais, V. Heine, C. Nex, and E. Salje, Phys. Rev. Lett. **66**, 2480 (1991).
[15] T. Onozuka, N. Ohnishi, and M. Hirabayashi, Metall. Trans. A **19**, 797 (1988).
[16] E. F. Fujita, Mater. Sci. Eng. A **127**, 243 (1990).
[17] J. van Landuyt, Phys. Status Solidi **6**, 957 (1964).
[18] M. Hirabayashi and S. Weissman, Acta Metall. **10**, 25 (1962).
[19] V. S. Arunachalain and R. S. Cahn, J. Met. Sci. **2**, 160 (1967).
[20] J. M. Pennison, A. Bourret, and P. Euren, Acta Metall. **19**, 1195 (1971).
[21] L. E. Tanner, Phys. Status Solidi **30**, 685 (1968).